

3D Analysis of Myocardial Perfusion from Vasodilator Stress Computed Tomography: Can Accuracy Be Improved by Iterative Reconstruction?

Victor Mor-Avi¹, Nadjia Kachenoura^{1,2}, Nicole M Bhave¹, Benjamin H Freed¹, Michael Vannier¹, Karin Dill¹, Roberto M Lang¹, Amit R Patel¹

¹University of Chicago Medical Center, Chicago, Illinois, USA

²Inserm, U678, Laboratoire d'Imagerie Fonctionnelle, 75013, Paris, France

Abstract

Computed tomography (CT) is an emerging tool to detect stress-induced myocardial perfusion abnormalities. We hypothesized that iterative reconstruction (IR) could improve the accuracy of the detection of significant coronary artery disease using quantitative 3D analysis of myocardial perfusion during vasodilator stress.

We studied 39 patients referred for CT coronary angiography (CTCA) who agreed to undergo additional imaging with regadenoson (Astellas). Images were acquired using 256-channel scanner (Philips) and reconstructed using 2 different algorithms: filtered back-projection (FBP) and IR (iDose7, Philips). Custom software was used to analyze both FBP and IR images. An index of severity and extent of perfusion abnormality was calculated for each 3D myocardial segment and compared to perfusion defects predicted by coronary stenosis >50% on CTCA.

Five patients with image artifacts were excluded. Ten patients with normal coronaries were used to obtain reference values, which were used to correct for x-ray attenuation differences among normal myocardial segments. Compared to the conventional FBP images, IR images had considerably lower noise levels, resulting in tighter histograms of x-ray attenuation. In the remaining 24 patients, IR improved the detection of perfusion abnormalities.

Quantitative 3D analysis of MDCT images allows objective detection of stress-induced perfusion abnormalities, the accuracy of which is improved by IR.

1. Introduction

The ability of multidetector computed tomography (MDCT) to detect stress-induced myocardial perfusion abnormalities is of increasing clinical interest as a potential tool for the combined evaluation of coronary stenosis and its physiological significance [1-5]. MDCT evaluation of myocardial perfusion is mostly qualitative,

involves selected 2D slices, and requires manual adjustment of contrast windows, both carrying the risk of missing small or less pronounced perfusion defects. Accordingly, we developed a technique for quantitative 3D analysis of myocardial perfusion from MDCT images, which takes into account the entire myocardium [6,7].

However, MDCT images obtained in overweight or obese patients are frequently of insufficient quality, which affects the interpretation of both coronary anatomy, and even more so myocardial perfusion during vasodilator stress, since stress imaging is usually performed with lower tube voltage to minimize radiation exposure [8].

Recently developed iterative reconstruction (IR) techniques, designed to reduce image noise [9], have been shown to improve the confidence in the interpretation of CT coronary angiography (CTCA) [10]. However, the utility of IR in stress CT perfusion imaging has not been systematically investigated. Accordingly, we designed this study to test the hypothesis that IR could improve the accuracy of the detection of stress-induced perfusion defects using our quantitative 3D analysis.

2. Methods

We studied 39 consecutive patients (age: 53±10 years, 26 males, body mass index: 30.3±6.6 kg/m²) who underwent clinically indicated CTCA and an additional scan during vasodilator stress. Patients with contraindications to CTCA, including known allergies to iodine, renal dysfunction, inability to perform a 10 sec breath-hold, and contraindications to beta-blockers or regadenoson, were excluded from the study. In addition, patients who had history of cardiothoracic surgery or pacemaker implantation were excluded.

Images were acquired using an MDCT system (256-channel iCT scanner, Philips). Imaging settings included: 270 ms gantry rotation time, slice thickness 0.625 mm and tube currents 600-1000 mA. Iodinated contrast agent was injected into a right antecubital vein and followed by a 20 ml chaser bolus.

Resting images were acquired according to a standard clinical CTCA protocol using prospective gating at a 75% phase of the cardiac cycle. Contrast doses varied between 65 and 90 ml, which were infused at rates of 5-6 ml/sec with tube voltages between 100 and 120 kV, depending on individual patient's characteristics.

After resting imaging was performed, regadenoson (Astellas) was administered (0.4 mg, i.v.) at least 15 min later to ensure contrast clearance. Regadenoson stress images were acquired using the following settings: tube voltage of 100 kV at 40% phase of the cardiac cycle, with prospective gating to minimize radiation exposure [8]. Patients received 50 ml of iodinated contrast agent at a rate of 4 ml/sec.

Resting images were reconstructed using the standard filtered back-projection (FBP) algorithm (Philips). CTCA reading was performed on the resting images by an experienced reader, whose interpretation of coronary anatomy included the determination of presence, location and extent of stenosis in percent of luminal narrowing. Narrowing >50% was considered as significant stenosis that would be expected to result in a perfusion defect during vasodilator stress. In addition, the specific location of stenosis, when detected on CTCA, was used to determine which myocardial segments would be affected.

Stress images were reconstructed using 2 different algorithms: standard FBP and IR (iDose7, Philips). Myocardial perfusion during regadenoson stress was analyzed from both FBP- and IR-reconstructed images using custom software for volumetric analysis described previously [6;7]. Briefly, following manual initialization of endo- and epicardial boundaries, the endo- and epicardial 3D surfaces were automatically estimated using the level-set technique [11]. The 3D region of interest confined between the endocardial and epicardial surfaces was identified as LV myocardium and divided into 16 3D wedge-shaped segments: 6 basal, 6 mid-ventricular, and 4 apical. Coronary arteries and contrast-filled intertrabecular spaces were excluded from the myocardial segments and papillary muscles and trabeculae were excluded from the LV cavity by setting thresholds on the histograms of x-ray attenuation [6;7].

X-ray attenuation in all LV slices from base to apex was used to generate a bull's eye display of myocardial attenuation normalized by mean LV cavity attenuation [12]. Unlike our previous study of fixed perfusion defects, in which the bull's eyes displayed transmural attenuation, in this study we created bull's eyes of subendocardial attenuation, to optimize the visualization of stress-induced perfusion defects.

In addition, for each myocardial segment, a quantitative index of extent and severity of perfusion abnormality, Q_h , was calculated from the histograms of x-ray attenuation (fig. 1) [6;7]. Briefly, this index is a mathematical product of the number of voxels with low attenuation in percent of the total volume of the segment

(reflecting the extent of the defect) and the difference between the attenuation in these voxels and the previously determined normal attenuation in the same anatomic location (reflecting the severity of the defect).

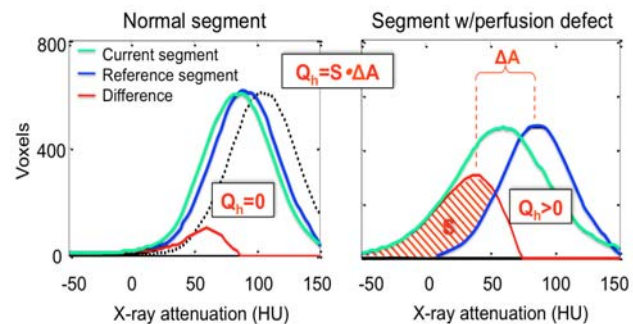


Figure 1. Quantification of extent and severity of myocardial hypoenhancement. Histograms of x-ray attenuation obtained in a segment with normal attenuation (left, green line) and in a segment with a fixed perfusion defect on SPECT (right, green line), shown with the adjusted reference histograms (blue lines). While for the normal segment, the difference between the histogram and the adjusted reference (left, red line) overlapped completely with the reference, the abnormal segment overlapped only partially with the adjusted reference (right, red line). The non-overlapping area, S , was used as a measure of the extent of hypoenhancement, and the distance between the peaks of the red and blue curves, ΔA , was used as a measure of the severity of the defect. The product $S \cdot \Delta A$ was defined as a combined index of extent and severity of perfusion abnormality.

To determine the ability of the index Q_h to classify segmental perfusion as normal or abnormal, ROC-derived threshold based classification of segments as normal or abnormal was compared to perfusion defects predicted by the presence and severity of coronary stenosis >50% in the corresponding artery on CTCA. Statistics of agreement (sensitivity, specificity, positive and negative predictive values and overall accuracy) were studied on a segment-by-segment, vascular territory and patient-by-patient basis. These comparisons were performed separately for FBP- and IR-reconstructed stress images, in order to determine the added value of IR for the detection of CAD.

3. Results

Overall, in the entire study group, 5 patients were excluded because of image artifacts. Of the remaining 34 patients, 10 patients with normal coronaries were used to obtain reference values, which were used to account for segmental heterogeneity due to anatomic location. The accuracy of detection of perfusion abnormalities caused by stenosis >50% was tested in the remaining 24 patients using analysis of FBP and separately IR images.

Stress IR images had considerably lower noise levels compared to the FBP images (fig. 2) in both the blood pool (SNR: 7.8 ± 3.0 for FBP vs. 11.8 ± 4.9 for IR, $p < 0.05$) and the myocardium (SNR: 3.0 ± 1.4 for FBP vs. 6.4 ± 2.4 for IR, $p < 0.05$).

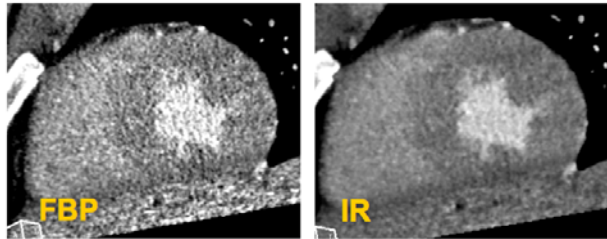


Figure 2. Example of a mid-ventricular short-axis image of the heart, reconstructed from the same MDCT dataset using standard filtered back-projection (FBP, left) and using the iterative reconstruction (IR) algorithm (right). Note the difference in image quality.

This improvement in image quality with the use of IR resulted in more uniform myocardial x-ray attenuation, as reflected by tighter histograms (fig. 3).

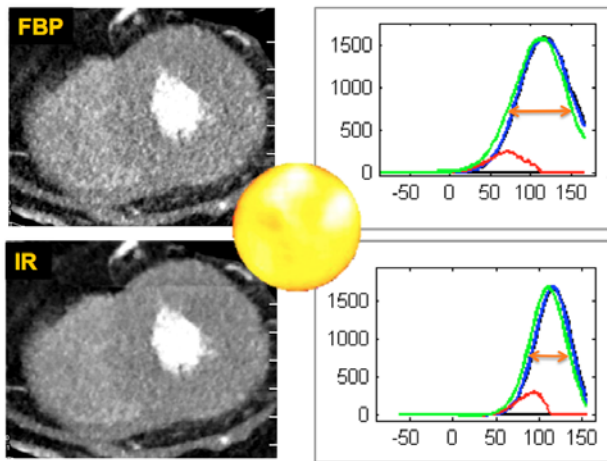


Figure 3. Example of short-axis images of the heart obtained in a patient with no significant coronary artery disease. Both images were reconstructed from the same MDCT dataset using standard FBP (top, left) and the IR algorithm (bottom, left). Also shown are the bull's eye display of myocardial attenuation from base to apex (center) and the histograms of x-ray attenuation (right) from one 3D segment. Note the difference in the width of the distribution curves between FBP and IR.

Figure 4 shows an example of images obtained in a patient with significant coronary stenosis. While a perfusion defect is noticeable in the LAD territory on both FBP and IR images as well as in the bull's eye, histograms of x-ray attenuation obtained from the FBP-reconstructed dataset failed to detect the perfusion defect. However, the same analysis applied to IR images, revealed a large perfusion defect of considerable extent.

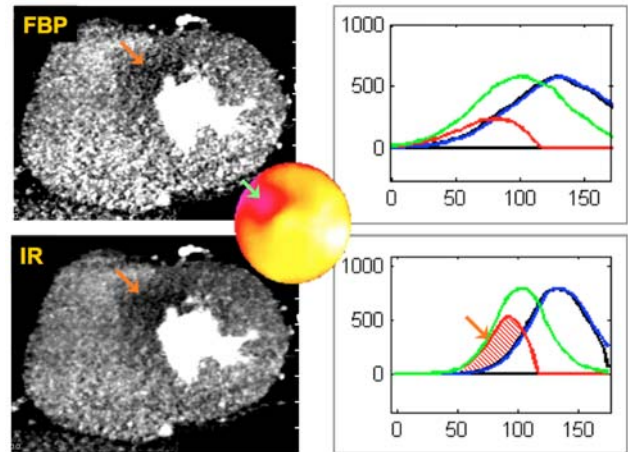


Figure 4. Example of images (in the same format as in figure 3) obtained in a patient with LAD stenosis $> 50\%$. Both FBP and IR images as well as the bull's eye show a perfusion defect in the antero-septal segment (arrows). Histograms of x-ray attenuation measured in this segment in the FBP-reconstructed dataset (top, right) did not show considerable non-overlapping area with the corresponding reference curve, i.e. did not detect a clear perfusion defect. In contrast, the same analysis applied to the IR images resulted in tighter histograms, revealing a large non-overlapping area with the reference histogram (dashed area), indicating a perfusion defect of considerable extent.

Of the 24 patients, 18 patients did not have significant stenosis on CTCA and thus were presumed to have normal perfusion in all myocardial segments. In contrast, the remaining 6 patients had stenosis $> 50\%$ in 8 coronary territories (6 left anterior descending artery, LAD, and 2 right coronary artery, RCA) and were expected to affect 41 myocardial segments (34 in the LAD territory and 7 in the RCA territory).

The detection of these perfusion defects using index Qh calculated by 3D segmental analysis of x-ray attenuation was improved by the use of IR (Table 1).

		Sensitivity	Specificity	PPV	NPV	Accuracy
By segment	FBP	0.54	0.75	0.21	0.93	0.73
	IR	0.66	0.79	0.28	0.95	0.78
By territory	FBP	0.75	0.72	0.25	0.96	0.72
	IR	0.88	0.78	0.33	0.98	0.79
By patient	FBP	0.83	0.39	0.31	0.88	0.50
	IR	1.00	0.56	0.43	1.00	0.67

Table 1. Diagnostic accuracy of the quantitative index of severity and extent of myocardial perfusion deficit derived by 3D analysis of cardiac CT images obtained in 24 patients undergoing regadenoson stress using FBP reconstruction versus IR, as determined by comparisons to CT coronary angiography findings. PPV, NPV – positive and negative predictive value.

4. Discussion

The results of our recent study [7] showed that myocardial segments affected by significant coronary stenosis had lower x-ray attenuation, but the variability in segmental attenuation caused by a variety of anatomical variables (e.g. body habitus) as well as technological factors (e.g. tube voltage, contrast infusion rates) did not always allow accurate detection of perfusion defects using our 3D analysis of myocardial perfusion from MDCT images. The use of the segmental index of perfusion abnormality has circumvented many of these issues and allowed better differentiation between normally perfused and hypoperfused segments. Nevertheless, the relatively low sensitivity reported in this recent study as a result of frequent false negative detections due to image noise, has motivated us to seek ways to further improve the sensitivity of our analysis by using the newly developed IR images.

We found that the use of IR for MDCT cardiac imaging during regadenoson stress was feasible and resulted in the majority of patients in images of improved quality, compared to the standard FBP (fig. 2). Specifically, this improvement manifested itself in higher SNR in IR datasets. As a result, IR images were found to have tighter distribution of x-ray attenuation values measured in the normally perfused myocardial tissue (fig. 3). The implication of this finding in the context of quantitative 3D analysis of stress perfusion was that IR improved the differentiation between normal and underperfused myocardium (fig. 4), and thus allowed more accurate detection of perfusion defects, as reflected by higher sensitivity, specificity, negative and positive predictive values and the overall accuracy (Table 1). Importantly, this improvement was evident across the board, on a segment, coronary territory and patient basis.

One limitation of this study is the small number of patients with perfusion defects, which reduces the confidence of our conclusions. This limitation stems from the fact that this was a sub-study of a larger study designed to test the usefulness of our 3D perfusion analysis in consecutive patients referred for cardiac CT for the evaluation of coronary artery disease. In this patient population, the incidence of stress-induced perfusion defects is quite low.

In summary, this is the first study to demonstrate that volumetric analysis of myocardial perfusion from MDCT images obtained using the newly developed iterative reconstruction during regadenoson stress in consecutive patients referred for CTCA can detect hypoperfused myocardium better than the same analysis when applied to the standard FBP reconstructed images. Although this methodology requires further validation, this study may have important implications on how MDCT stress perfusion images should be reconstructed and analyzed.

Acknowledgements

This study was funded by a research grant from Astellas Global Development.

References

- [1] Techasith T, Cury RC. Stress Myocardial CT perfusion. *J Am Coll Cardiol Img* 2011; 4:905-16.
- [2] George RT, et al. Multidetector computed tomography myocardial perfusion imaging during adenosine stress. *J Am Coll Cardiol* 2006; 48:153-60.
- [3] Blankstein R, et al. Adenosine-induced stress myocardial perfusion imaging using dual-source cardiac computed tomography. *J Am Coll Cardiol* 2009; 54:1072-84.
- [4] Cury RC, et al. Dipyridamole stress and rest myocardial perfusion by 64-detector row computed tomography in patients with suspected coronary artery disease. *Am J Cardiol* 2010; 106:310-5.
- [5] Okada DR, et al. Direct comparison of rest and adenosine stress myocardial perfusion CT with rest and stress SPECT. *J Nucl Cardiol* 2010; 17:27-37.
- [6] Kachenoura N, et al. Volumetric quantification of myocardial perfusion using analysis of multi-detector computed tomography 3D datasets: comparison with nuclear perfusion imaging. *Eur Radiol* 2010; 20:337-47.
- [7] Mor-Avi V, et al. Quantitative three-dimensional evaluation of myocardial perfusion during regadenoson stress using multidetector computed tomography. *J Comput Assist Tomogr* 2012; 36:443-9.
- [8] Patel AR, et al. Detection of myocardial perfusion abnormalities using ultra-low radiation dose regadenoson stress multidetector computed tomography. *J Cardiovasc Comput Tomogr* 2011; 5:247-54.
- [9] Utsunomiya D, et al. Effect of hybrid iterative reconstruction technique on quantitative and qualitative image analysis at 256-slice prospective gating cardiac CT. *Eur Radiol* 2012; 22:1287-94.
- [10] Noel PB, et al. Initial performance characterization of a clinical noise-suppressing reconstruction algorithm for MDCT. *Am J Roentgenol* 2011; 197:1404-9.
- [11] Corsi C, et al. Volumetric quantification of global and regional left ventricular function from real-time three-dimensional echocardiographic images. *Circulation* 2005; 112:1161-70.
- [12] Kachenoura N, et al. Value of multidetector computed tomography evaluation of myocardial perfusion in the assessment of ischemic heart disease: comparison with nuclear perfusion imaging. *Eur Radiol* 2009; 19:1897-905.

Address for correspondence.

Victor Mor-Avi
University of Chicago Medical Center MC5084
5841 S. Maryland Ave., Chicago, IL 60637, U.S.A.
vmoravi@bsd.uchicago.edu